A Single-Switched High-Switching-Frequency Quasi-Resonant Flyback Converter

Chong Wang, Shen Xu, Weidong Shen, Shengli Lu, and Weifeng Sun, *Senior Member, IEEE*

***Abstract*—The demand of miniaturization of power systems has accelerated the research on high-switching-frequency power converters. A single-switched quasi-resonant flyback converter that features low switching loss and low switching noise at high switching frequency is investigated in this paper. In order to realize near fully soft switching, a resonant inductor of primary side and a resonant capacitor of secondary side are utilized to recycle the transformer leakage energy and realize zero-current switching (ZCS) at turn OFF and valley switching (VS) at turn ON of the primary switch, and ZCS at turn OFF of diode. The VS is utilized based on the resonance between the resonant inductor and the equivalent switch drain capacitor. In the closed-loop control, a pulse frequency modulation mode with time fluctuation of switching period is implemented to realize VS at turn ON of switch and an ON–OFF control mode is utilized to improve the overall efficiency. Low cost, low losses, and low switching noise are all realized in the proposed prototype. The proposed concept has been validated on a 1 MHz 12 V/3 A prototype with 80 V dc input. The peak efficiency is 90.3% in the ON–OFF mode by using GaN device without synchronous rectification.**

***Index Terms*—Flyback converter, high switching frequency, quasi resonant, single switched, valley switching (VS), zero-current switching (ZCS).**

I. Introduction

FLYBACK converter topology is widely used in low-power dc–dc supplies. Nowadays, power density is becoming an important factor for evaluating these converters. Increasing the switching frequency is a potential solution to improve power density. In higher-switching-frequency converters, lower inductance, smaller capacitance, and transformer of less turns and smaller cores are used.

Single-switched isolated converters have the advantages of simple control and high stability. However, at high switching frequency, recycling the leakage energy of the transformer, reducing the switching loss, and reducing the switching noise must be maintained. Applying soft switching, valley switching

Manuscript received June 27, 2018; revised September 10, 2018 and October 27, 2018; accepted November 26, 2018. Date of publication December 4, 2018; date of current version June 10, 2019. This work was supported in part by the National Nature Science Foundation of China under Grant 61674033, in part by the Natural Science Foundation of Jiangsu Province under Grant BK20161148, and in part by Key Research & Development Plan of Jiangsu Province under Grant BE2017083. Recommended for publication by Associate Editor X. Ruan. *(Corresponding author: Weifeng Sun.)*

The authors are with the National ASIC System Engineering Research Center, Southeast University, Nanjing 210096, China (e-mail:

a single-switch quasi-resonant forward converter is realized by adding an inductor and a capacitor. The energy of leakage inductance is recycled. And the switching loss is reduced as ZCS turn OFF of the switch and ZCS turn OFF of diode are accomplished. *di/dt* value is attenuated. But the turn ON of switch is still hard switching leading to large *dv/dt* value and large switching loss. The switching loss increases linearly with the switching frequency. Thus, high efficiency cannot be maintained and the maximum switching frequency is around 300 kHz. In addition, large transformer volume is introduced by the large magnetizing inductance. In [13], an improved flyback converter is proposed to realize power factor correction and ZCS turn OFF of switch. One inductor, two capacitors, and two diodes are required. The leakage energy of the transformer is recycled. However, the turn ON of the switch is still hard switching. The maximum switching frequency is also around 300 kHz.

This paper proposes a single-switched high-switching-frequency quasi-resonant flyback converter. A resonant inductor and a resonant capacitor are added to the flyback converter, which eliminates the RCD snubber network for leakage energy dissipation. ZCS turn OFF and VS turn ON of switch and ZCS turn OFF of diode are achieved. Based on the resonance between the resonant inductor and the equivalent drain capacitor, VS turn ON of the switch is applied. With VS at high switching frequency, the switching loss is reduced and *dv/dt* value is attenuated. In closed-loop control, a pulse frequency modulation (PFM) mode with time fluctuation is used to realize VS turn ON of switch and an ON–OFF mode is proposed to improve the overall efficiency. Besides, gallium nitride (GaN) switch is also exploited, which enables higher switching frequencies at lower switching losses compared to silicon power switches. A 1 MHz 12 V/3 A prototype with 80 V dc input voltage is applied to verify the proposed analysis.

This paper is organized as follows. Section II introduces its detailed operation of the proposed topology. Section III presents a general design procedure. Section IV discusses several control methods for closed-loop control. Section V verifies the proposed prototype and the measured results. The paper is concluded in Section VI.

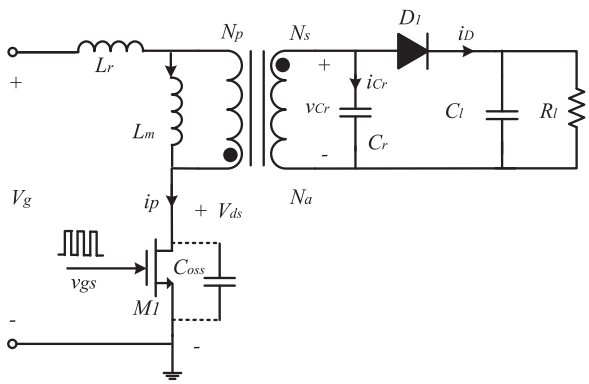

Fig. 1. Proposed quasi-resonant flyback converter.

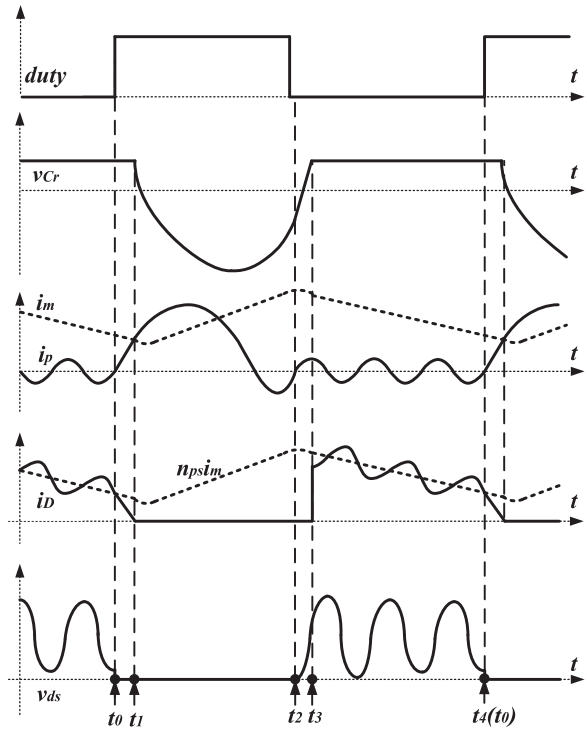

Fig. 2. Steady-state waveforms of the proposed QR flyback converter.

II. Quasi-Resonant Flyback Converter With ZCS and VS

The schematic of the proposed quasi-resonant flyback converter is shown in Fig. 1. Compared to traditional flyback converter, the RCD snubber circuit is eliminated. A resonant inductor L_r and a resonant capacitor C_r are added. In Fig. 1, the transformer leakage inductance and the resonant inductance are included in L_r.

In one switching cycle, there are four time intervals as shown in Fig. 2. $v_{\rm Cr}$ is the voltage of capacitor C_r. i_p is the primary winding current of the transformer. i_m is the magnetizing current of the transformer. i_D is current of output diode $\rm D_1$, and $v_{\rm ds}$ is the switch drain source voltage. ZCS turn OFF, and VS turn ON of switch and ZCS turn OFF of diode are realized. $\rm N_p$ and N_s are the turn's number of primary winding and secondary winding of the transformer. The schematic and the equivalent circuit of the four intervals are shown in Fig. 3.

Mode a. (t_0–t_1): The steady-state cycle starts at $\rm t_0$ when the switch $\rm M_1$ is turned ON and the output diode $\rm D_1$ is still ON. $\rm t_0$ is the time when the drain-source voltage ($v_{\rm ds}$) is at its valley, i.e., VS at turn ON for low switching losses. The equivalent circuit can be shown in Fig. 3(a1).

The voltage of resonant capacitor C_r ($v_{\rm Cr}$) is equal to the sum of the output voltage V_o and the forward voltage of diode $\rm D_1$ (V_f). Assuming that the output diode is an ideal device (V_f is zero), the increasing slope of i_p and the decreasing slope of i_D can be expressed as in (1). V_g is the input voltage. L_m is the magnetization inductance of the transformer and i_m is the magnetization inductance current. $n_{\rm ps}$ represents the turn's ratio between the primary winding and the secondary winding.

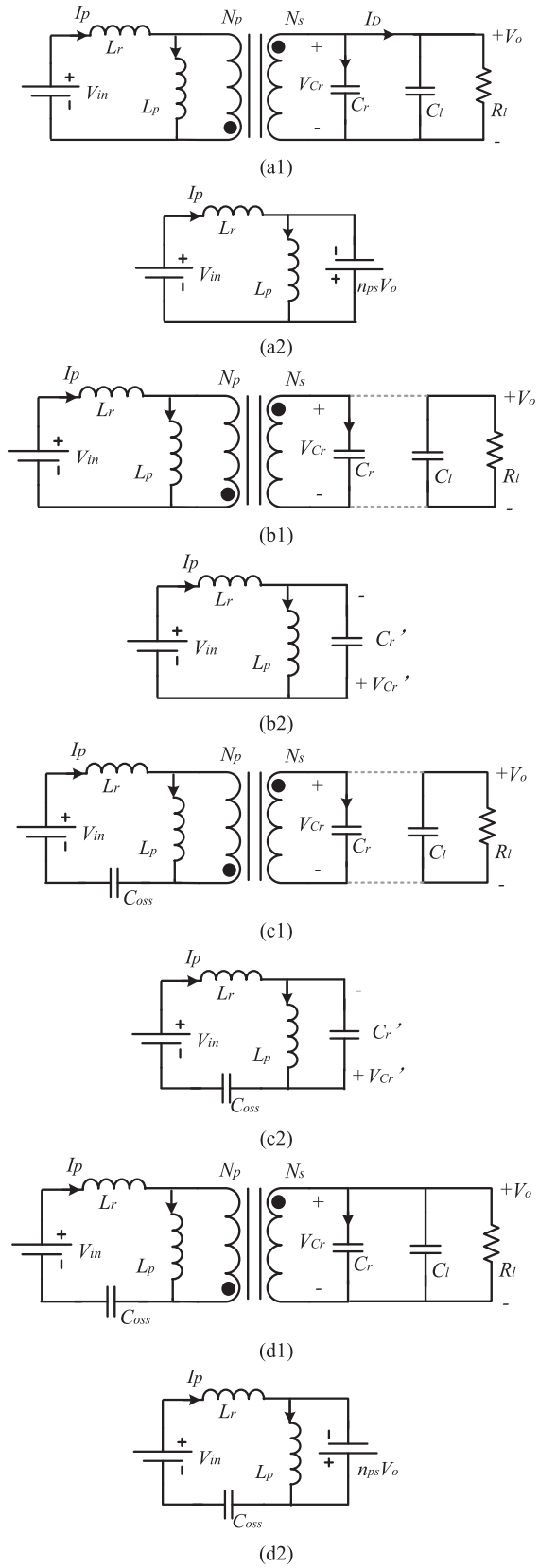

Fig. 3. Steady-state operating modes and respective equivalent circuits. (a1) Equivalent circuit in t_{10}. (a2) Simplified circuit in t_{10}. (b1) Equivalent circuit in t_{21}. (b2) Simplified circuit in t_{21}. (c1) Equivalent circuit in t_{32}. (c2) Simplified circuit in t_{32}. (d1) Equivalent circuit in t_{43}. (d2) Simplified circuit in t_{43}.

The primary current i_p increases linearly as the voltage across L_r is constant. The magnetizing current i_m decreases linearly as the voltage across the secondary winding is minus and constant. Thus, the current flow through output diode D_1 (i_D) decreases linearly. This period ends at t_1 when i_D reaches zero, and the diode D_1 is turned OFF

$$\begin{cases} L_r \frac{di_p(t)}{dt} = V_g + n_{\rm ps} V_o \\ L_m \frac{di_m(t)}{dt} = -n_{\rm ps} V_o \\ i_D(t) = n_{\rm ps}(i_m(t) - i_p(t)). \end{cases} \tag{1}$$

Mode b. (t_1–t_2): This mode starts at t_1. In this period, the switch is turned ON and the output diode D_1 is turned OFF. The equivalent circuit is shown in Fig. 3(b1).

L_r, L_m, and C_r start to resonate in this period. For simplicity, the circuit is simplified as Fig. 3(b2). C_r' is the corresponding capacitor of C_r, and $v_{\rm Cr}$' is the corresponding voltage of $v_{\rm Cr}$. C_r' and $v_{\rm Cr}$' can be expressed in (2).

i_m, i_p, and $v_{\rm Cr}$' can be calculated as in (3). The analytical expression of i_m, i_p, and $v_{\rm Cr}$' can be expressed in (4). i_p can be seen as the sum of a linearly increasing current and a sine wave current. When the amplitude of this sine wave current is large enough, zero current can be obtained, and ZCS turn OFF of switch can be realized. i_m can also be seen as the sum of a linearly increasing current and a sine wave current. $v_{\rm Cr}$ can be seen as the sum of a cosine wave voltage and a minus dc voltage. This period ends at t_2 when i_p increases from below zero current to above zero current. The time length of this period t_{21} is larger than half the resonant period π/w_1, but smaller than one resonant period $2\pi/w_1$. Thus at t_2, $v_{\rm Cr}$ is increasing, but lower than V_o

$$C\prime_r = \frac{C_r}{n_{\rm ps}^2},\ v\prime_{\rm Cr} = n_{\rm ps} v_{\rm Cr} \tag{2}$$

$$\begin{cases} L_m \frac{di_m(t)}{dt} = -v'_{\rm Cr}(t) \\ L_r \frac{di_p(t)}{dt} = V_g + v'_{\rm Cr}(t) \\ C\prime_r \frac{dv'_{\rm Cr}(t)}{dt} = i_m(t) - i_p(t) \end{cases} \tag{3}$$

$$\begin{cases} i_m(t-t_1) = -\frac{v'_{\rm Cr}(t_1)+V_{ge}}{w_1 L_m}\sin(w_1(t-t_1)) \\ \qquad\qquad + \frac{V_g}{L_m+L_r}(t-t_1) + i_m(t_1) \\ i_p(t-t_1) = \frac{v'_{\rm Cr}(t_1)+V_{ge}}{w_1 L_r}\sin(w_1(t-t_1)) \\ \qquad\qquad + \frac{V_g}{L_m+L_r}(t-t_1) + i_m(t_1) \\ v'_{\rm Cr}(t-t_1) = (v'_{\rm Cr}(t_1) + V_{ge})\cos(w_1(t-t_1)) - V_{ge} \end{cases}$$

$$V_{ge} = \frac{L_m}{L_m + L_r} V_g,\ w_1 = \sqrt{\frac{1}{C\prime_r}\left(\frac{1}{L_m} + \frac{1}{L_r}\right)}. \tag{4}$$

Mode c. (t_2–t_3): This mode starts at t_2. In this period, the switch is turned OFF and the output diode is OFF. The equivalent circuit is shown in Fig. 3(c1). L_r, L_m, C_r, and $C_{\rm oss}$ start to resonate. $C_{\rm oss}$ is equivalent drain source capacitance. The circuit

is simplified as in Fig. 3(c2). i_m, i_p, and $v_{\rm Cr}$' can be calculated as in (5). In this period, i_p can be neglected compared to the magnetizing current i_m. Thus, $C_{\rm r}'$ is charged by the magnetizing current $i_{\rm m}$ resulting in the fast increase of $v_{\rm Cr}$'. This period ($\rm t_{32}$) is very short and variation of i_m is small.

In $\rm t_{32}$ period, there are two resonating frequencies, whose analytical expressions are shown in (6). The higher switching frequency w_{21} is mainly determined by L_r and $C_{\rm oss}$, the lower frequency w_{22} is determined by L_m and C_r'. The switch drain voltage ($v_{\rm ds}$) is composed by one dc voltage, a resonant voltage of frequency w_{21}, and a resonant voltage of frequency w_{22}. The lower frequency element is always small and can be ignored. When $v_{\rm Cr}$ reaches the output voltage V_o at $\rm t_3$, this mode ends and the output diode $\rm D_1$ is turned ON

$$\begin{cases} L_m \frac{di_m(t)}{dt} = -v\prime_{Cr}(t) \\ L_r \frac{di_p(t)}{dt} = V_g + v\prime_{Cr}(t) - v_{ds}(t) \\ C\prime_r \frac{dv\prime_{Cr}(t)}{dt} = i_m(t) - i_p(t) \\ C_{\rm oss} \frac{dv_{ds}(t)}{dt} = i_p(t) \end{cases} \tag{5}$$

$$w_{22} = \sqrt{\frac{b-\sqrt{b^2-4a}}{2a}} \approx \frac{1}{\sqrt{L_m C\prime_r}},$$

$$w_{22} = \sqrt{\frac{b-\sqrt{b^2-4a}}{2a}} \approx \frac{1}{\sqrt{L_m C\prime_r}}$$

$$a = L_m C\prime_r L_r C_{\rm oss},\ b = L_r C_{\rm oss} + L_m C\prime_r + L_m C_{\rm oss}. \tag{6}$$

Mode d. (t_3–t_4): This mode starts at $\rm t_3$. In this period, the switch is turned OFF and the output diode is turned ON. The equivalent circuit is shown in Fig. 3(d1). The voltage on the secondary winding of the transformer is clamped at the output voltage V_o. Thus, the magnetizing current i_m decreases linearly and the transformer energy is transferred to the output capacitor. i_m, i_p, $v_{\rm ds}$, and $v_{\rm Cr}$' can be calculated as in (7). L_r and $C_{\rm oss}$ resonant in this period. The resonant frequency w_3 is shown in (8). This interval ends at $\rm t_4$. $v_{\rm ds}$ is at its valley and the switch is turned ON. Assuming the resonance of $v_{\rm ds}$ has no attenuation, the valley voltage of $v_{\rm ds}$ is near zero. Near ZVS (VS turn ON of switch) will be acquired. The switching loss will be reduced greatly

$$\begin{cases} L_m \frac{di_m(t)}{dt} = -n_{ps} V_o \\ L_r \frac{di_p(t)}{dt} = V_g + n_{ps} V_o - v_{ds}(t) \\ C_{oss} \frac{dv_{ds}(t)}{dt} = i_p(t) \\ v\prime_{Cr}(t) = n_{ps} V_o \end{cases} \tag{7}$$

$$w_3 = \sqrt{\frac{1}{L_r C_{\rm oss}}}. \tag{8}$$

Based on the above analysis, ZCS turn OFF and VS turn ON of switch and ZCS turn OFF of diode are realized in the proposed single-switched quasi-resonant flyback converter. The converter efficiency will be improved, and *dv/dt* and *di/dt* values will be reduced.

III. Design of the Converter

From the above analysis, ZCS turn ON and VS turn OFF of switch is realized in the proposed single-switched quasi-resonant flyback converter.

A. Converter Behavior

In Mode b and c, the magnetization current i_m increases. In Mode a and d, the magnetization current decreases. Comparing to traditional flyback converter, Mode b and c is the equivalent switch ON period $t_{\rm on}$. $t_{\rm on}$ can be seen as equal to $\rm t_{31}$($\rm t_{31} = t_3 - t_1$). Mode a and d can be seen as the equivalent switch OFF period $t_{\rm off}$. The equivalent duty ratio $D_{\rm eq}$ can be expressed in the following:

$$t_{\rm on} = t_{21} + t_{32},\ t_{\rm off} = t_{10} + t_{43},\ D_{\rm eq} = \frac{t_{\rm on}}{t_{\rm on} + t_{\rm off}}. \tag{9}$$

During $t_{\rm on}$ period, the average voltage of $v_{\rm Cr}$ in Mode b and c is nearly equal to $-L_m V_g/(n_{\rm ps}(L_m + L_r))$ based on (4). During $t_{\rm off}$ period, $v_{\rm Cr}$ is equal to the output voltage. Based on volt-second balance principle, the equivalent duty ratio $D_{\rm eq}$ can be approximated as in (10). When $D_{\rm eq}$ is set, the turn's ratio will be determined. As too small or too large duty ratio will lead to large peak current of primary winding current i_p or diode current i_D, $D_{\rm eq}$ is set between 0.4 and 0.6. Usually, $D_{\rm eq}$ is set around 0.5

$$D_{\rm eq} = \frac{n_{\rm ps} V_o}{V_g L_m/(L_m + L_r) + n_{\rm ps} V_o}. \tag{10}$$

When the equivalent duty ratio $D_{\rm eq}$ is set, as L_r is much smaller than L_m, $D_{\rm eq}$ is nearly equal to $n_{\rm ps} V_o/(V_g + n_{\rm ps} V_o)$ and the turn's ratio can be obtained accordingly. After L_r and L_m is obtained, the accurate turn's ratio can be reobtained based on (10).

After the turn's ratio is set, the average magnetizing current will be calculated as I_m in (11). I_o is the output current. As $D_{\rm eq}$ is nearly constant, when the output power increases, I_m increases. The maximum value of I_m is $I_{m\_\max}$ which can be calculated from (12). $I_{\rm av\_in}$ is the input average current which can be acquired from (13). V_g is the input voltage. $\eta_{\rm eff}$ is the efficiency of the converter at full load

$$I_o = \frac{1}{T_s}\int_0^{T_s} i_D(t)dt \approx n_{\rm ps} I_m (1 - D_{\rm eq}) \tag{11}$$

$$I_{\rm av\_in} = I_{m\_\max} D_{\rm eq} \tag{12}$$

$$P_{o\max} = V_o I_o = \eta_{\rm eff} P_{in} = \eta_{\rm eff} V_g I_{\rm av\_in}. \tag{13}$$

Referring to (7), the maximum voltage at the drain node of the switch $V_{\rm ds\_max}$ can be approximated in (14) while the attenuation of the resonance is not considered. It is determined by the input voltage V_g, the output voltage V_o, and the transformer turn's ratio $n_{\rm ps}$. $V_{\rm ds\_max}$ must be guaranteed to be lower than the maximum

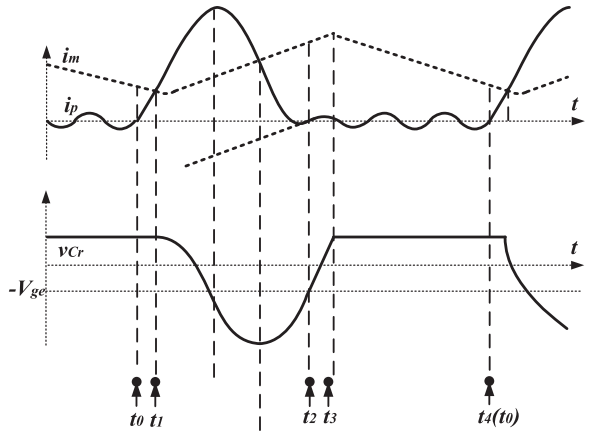

Fig. 4. Critical condition of the proposed method.

drain source voltage of the switch

$$V_{\mathrm{ds\_max}} = 2(V_g + n_{\mathrm{ps}} V_o). \tag{14}$$

B. Design Procedure

If ZCS turn OFF of switch is achieved when the average magnetizing current I_m is equal to its maximum value Im_{max}, ZCS turn OFF of switch can be guaranteed when I_m is smaller than $I_{m\_\max}$. Fig. 4 shows this critical condition of the proposed converter, in which the time length of the negative current interval of i_p in Mode b nears zero and the output power in this condition should be equal to or larger than the maximum output power. The parameter design would be committed in this condition.

1) Parameters Design: When the switching frequency and the equivalent duty ratio D_{eq} is set, t_{on} can be acquired from (9). Considering (4), the length of Mode b (t_{21}) is three quarters of the resonant period in the critical condition. t_{21} can be expressed in (15). The length of Mode c (t_{32}) in the critical condition is also calculated as in (16). The total length of the two periods (t_{on}) is calculated as in (17)

$$t_{21} = \frac{3\pi}{2}\sqrt{C\prime_r \frac{L_m L_r}{L_m + L_r}} \tag{15}$$

$$t_{32} = \sqrt{C\prime_r \frac{L_m L_r}{L_m + L_r}} \tag{16}$$

$$t_{\mathrm{on}} = t_{31} = t_{21} + t_{32} = \frac{3\pi + 2}{2}\sqrt{C\prime_r \frac{L_m L_r}{L_m + L_r}} = D_{\mathrm{eq}} T_s. \tag{17}$$

In Mode b, the input current i_p can be re-expressed as in (18). At t_2, as in Fig. 4, i_p is equal to zero, thus (19) is obtained. i_{m1} is the abbreviation of magnetizing current of i_m at t_1. Referring to (18), the input average current $I_{\mathrm{av\_in}}$ can be derived in (20). Considering energy conservation, $I_{\mathrm{av\_in}}$ can also be calculated in (13). Considering (19) and (20), A and k can be obtained as in (21). Based on (18), L_r, L_m, and C_r can be calculated from the given values of A and k. As $I_{\mathrm{av\_in}}$, T_s, t_{21} and t_{31} already acquired from the above design, only i_{m1} not determined. Thus, L_r, L_m, and C_r will vary with i_{m1}

$$i_p(t - t_1) = A\sin\left(w_1(t - t_1)\right) + k(t - t_1) + i_{m1}$$

$$A = \frac{n_{\mathrm{ps}} V_o + V_{ge}}{w_1 L_r}$$

$$k = \frac{V_g}{L_m + L_r} \tag{18}$$

$$i_p(t_2) = -A + kt_{21} + i_{m1} = 0 \tag{19}$$

$$I_{\mathrm{av\_in}} = \frac{1}{T_s}\int_{t_0}^{t_4} i_p(t)dt \approx \frac{1}{T_s}\int_{t_1}^{t_3} i_p(t)dt$$

$$= \frac{1}{T_s}\left(i_{m1} t_{21} + \frac{k}{2} t_{21}^2 + t_{32}\right)$$

$$= \frac{1}{T_s}\left(A t_{31} - \frac{k}{2} t_{21}^2\right) \tag{20}$$

$$\begin{cases} k = \dfrac{I_{\mathrm{av\_in}} T_s - i_{m1} t_{31}}{t_{21} t_{31} - t_{21}^2/2} \\ A = k t_{21} + i_{m1} \end{cases}. \tag{21}$$

After L_r, L_m and C_r are acquired, the turn's ratio of the transformer n_{ps} can be obtained. Based on the analysis in Section II, the voltage of the resonant capacitor v_{Cr} can be expressed as in (22). Based on volt-second balance principle, the integration of v_{Cr} in one switching period is zero as in (23), and the accurate value of the turn's ratio n_{ps} can be obtained as in (24)

$$\begin{cases} v'_{cr}(t - t_0) = n_{\mathrm{ps}} V_o, t_0 \le t < t_1 \\ v'_{cr}(t - t_1) = (n_{\mathrm{ps}} V_o + V_{ge})\cos\left(w_1(t - t_1)\right) - V_{ge}, t_1 \le t < t_2 \\ v'_{cr}(t - t_2) = -V_{ge} + \frac{n_{\mathrm{ps}} V_o + V_{ge}}{t_{32}}(t - t_2), t_2 \le t < t_3 \\ v'_{cr}(t - t_3) = n_{\mathrm{ps}} V_o, t_3 \le t < t_4 \end{cases} \tag{22}$$

$$\int_{t_o}^{t_4} v'_{\mathrm{cr}}(t)dt = -\frac{n_{ps} V_o}{2w_1} - \frac{3\pi + 3}{2w_1} V_{ge} + n_{\mathrm{ps}} V_o \frac{T_s}{2} = 0 \tag{23}$$

$$n_{ps} = \frac{3\pi + 3}{2w_1} V_{ge} / \left(V_o \frac{T_s}{2} - \frac{V_o}{2w_1}\right). \tag{24}$$

When i_{m1} is determined, L_m, L_r, C_r, and n_{ps} will be calculated based on (18), (21), and (24). There are many choices of the converter parameters when i_{m1} varies. The power loss calculation of different turn's ratio n_{ps} is shown in Fig. 5. The total power loss is at its minimal value when n_{ps} is equal to 4.72 (when i_{m1} is equal to 0.76 A). For simplicity, n_{ps} is taken as 4.5 (when i_{m1} is equal to 0.54 A). The primary winding turn's number N_p and the secondary winding turn's number N_s of the planar transformer are 9 and 2. When n_{ps} is equal to 4.5, as in Fig. 6, L_m, L_r, and C_r can be determined. L_m is 21.4 μH, L_r is 5.2 μH, and C_r is 30 pF.

2) Transformer Design: Based on the above analysis, the maximum magnetizing current $i_{m\max}$ of the transformer is 2.51 A. The maximum flux density $B_{\max}$ can be applied to determine the turn's number of the transformer as in (25). N_p is the primary turn's number; A_e is effective area of the planar transformer core. The primary winding turns is nine and the sec-

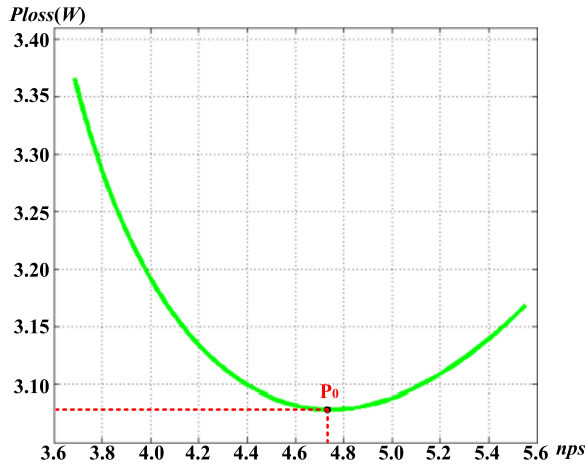

Fig. 5. Relationship between the power loss and the transformer turn's ratio.

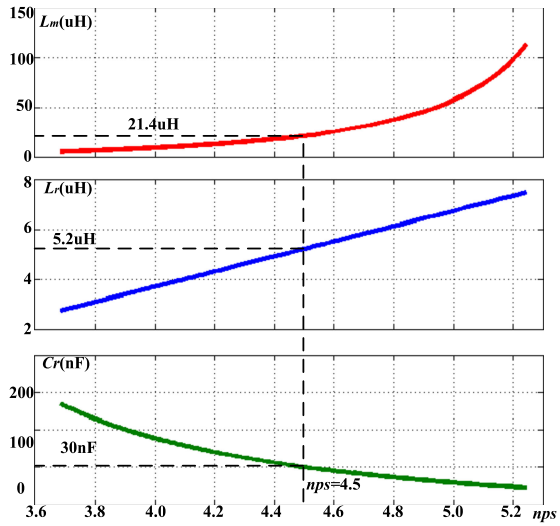

Fig. 6. Relationship between different parameters.

ondary winding turns is two. The ER23/3.6/13 core from Ferroxcube Corporation is chosen due to its large cross-sectional area, and window width and core of 3f46 material is used as its low core loss at high switching frequency. The detailed description of the transformer is shown in Fig. 7. Three printed circuit board (PCB) boards of four layers are stacked to form the transformer windings. The primary winding turns number of the top layer, the middle layer, and the bottom layer are 3.5, 3.5, and 2, and these primary windings of three layers are series connected. The secondary winding turns number of the three layers are all equal to two. These secondary winding of three layers are parallel connected

$$B_{\max} = \frac{L_m I_{m\max}}{N_p A_e}. \tag{25}$$

IV. Control of the Proposed Converter

After the parameters are set, the closed-loop control of the proposed converter should be considered. Based on (10), when

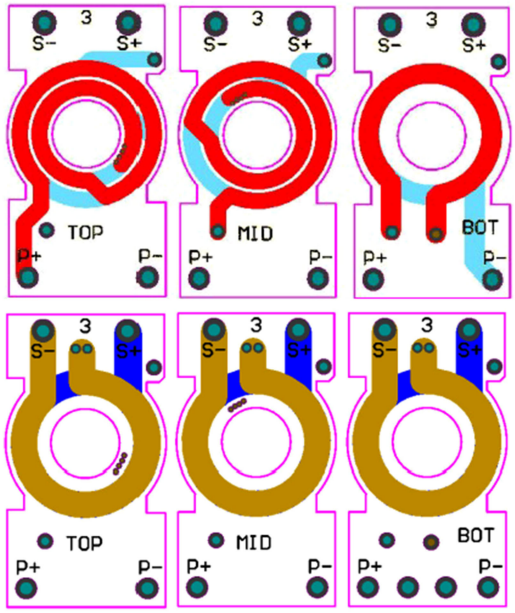

Fig. 7. Transformer construction. Core: ER13/3.6/13, core material 3f46.

the input and output are set, the stable equivalent duty ratio $D_{\text{eq\_}s}$ and the stable switching period t_{s_s} are acquired.

A. PFM Control Modes

As analyzed above, the equivalent switch-ON time t_{on} is determined by the initial magnetizing current at t_1 (i_{m1}), only the switch period t_s can be modulated in closed-loop control. When the load changes from light to heavy, the average magnetizing current I_m needs to be improved to maintain constant output voltage. I_m is improved by reducing the switching period t_s. When the load changes from heavy to light, the switching period t_s is improved to reduce I_m and reduce the power transferred to the output. Thus, in closed-loop control, the switching period is used to modulate the average magnetizing current I_m and modify the output power.

In Fig. 8(a), the switching period *ts* is used to realize constant output control with PFM mode. While the control is stable, the switching period *ts* is stable. As the resonance period tvalley in Mode d determined by Lr and Coss is unchanged, VS turn ON of switch cannot be guaranteed in PFM mode. In Fig. 8(a), the switch is turned ON between the (n)th valley and the (n+1)th valley of the switch drain voltage (v_{ds}). And the switching loss cannot be ignored. Thus, a fluctuation of the switching period is introduced in PFM mode shown in Fig. 8(b). The switch is turned ON at the closest valley of v_{ds} near the end of the given switching period *ts*. Assuming that the time length between the (n)th valley of v_{ds} and the switch ON interval is Δtvalley. If Δtvalley is lower than half of tvalley, the switch will be turned ON at the (n) th valley of v_{ds}. Otherwise, the switch will be turned ON at the (n + 1)th valley of v_{ds}. VS turn ON of switch is realized and the switching loss is greatly reduced. tvalley is calculated by comparing the primary winding current *ip* to zero current. We defined this improved PFM mode as PFM mode with time fluctuation.

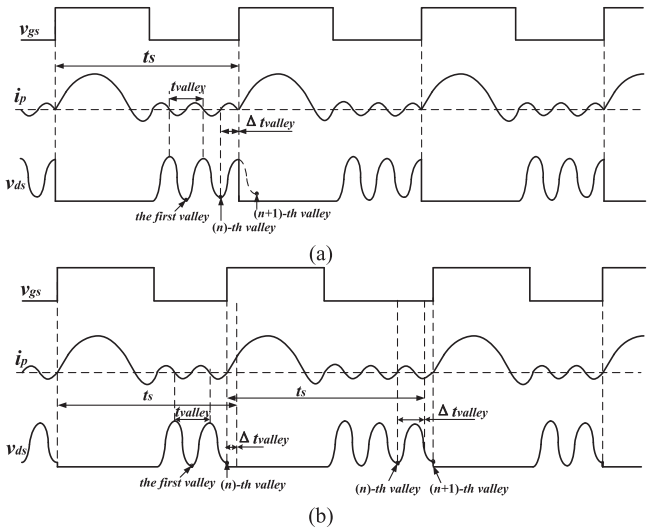

Fig. 8. Two PFM control methods of the proposed converter. (a) Normal PFM mode. (b) PFM mode with fluctuation of switching period.

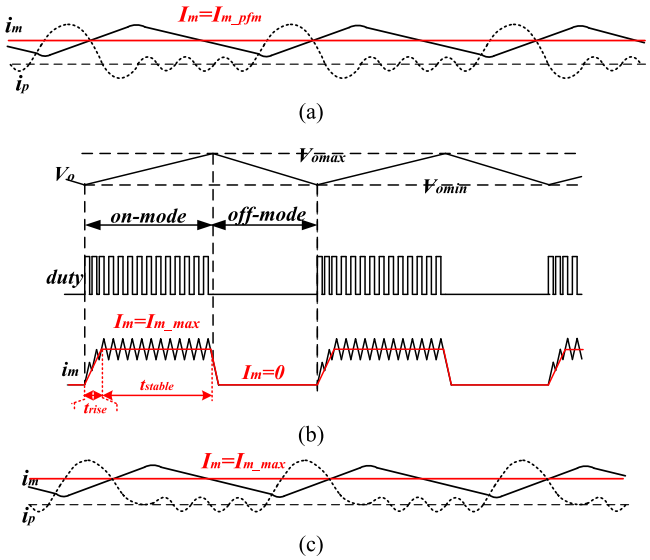

Fig. 9. ON–OFF mode using PFM mode with fluctuation of switching period. (a) Waveform of PFM mode with fluctuation. (b) Waveform of ON–OFF mode. (c) Waveform of ON mode.

B. ON–OFF Control Mode

Assuming that the average magnetizing current I_m is equal to I_{m_pfm} in PFM mode with fluctuation of switching period, I_{m_pfm} is smaller than or equal to its maximum value $I_{m\_\max}$. To reduce the power loss further, ON–OFF mode is applied as shown in Fig. 9(b). During ON mode, the average magnetizing current I_m is equal to $I_{m\_\max}$. The output voltage V_o will increase during ON mode as the input power is larger than the output power. When V_o reaches its upper limit $V_{o\max}$, OFF mode is used and the switch keeps OFF. No energy is transferred to the output and the output voltage V_o decreases. When V_o is lower than the lower limit $V_{o\min}$, ON mode will be activated. In ON mode, I_m is first improved from zero to $I_{m\_\max}$ during t_{rise} period. In t_{stable} period, I_m is maintained at $I_{m\_\max}$.

TABLE I
PARAMETERS OF THE PROPOSED PROTOTYPE

Quantity	Values	Remarks
Input voltage	V_g= 80 V	--
Output voltage	V_o=12 V	--
Output current	I_o=3 A	--
Transformer turns	N_p:N_s=9:2	--
Transformer core	ER23/3.6/13	3f46 material
Primary inductance	L_m=22 uH	--
Resonant inductor	L_r=5.2 uH	--
Resonant capacitor	C_r=30 nF	--
GaN-HEMT	GS66504	--

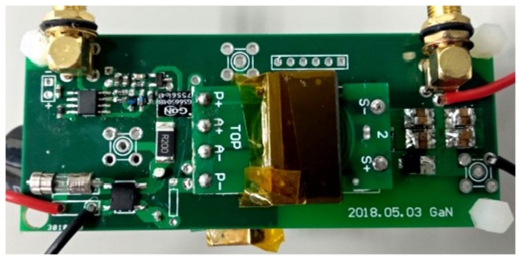

Fig. 10. Test board of the proposed topology.

The equivalent switching frequency will be reduced in ON–OFF mode. The switching loss, the conduction loss, the core loss, and the diode conduction loss are all reduced leading to the reduction of total power loss. The total efficiency is improved compared to the two previous PFM control modes.

The closed-loop control methods of the proposed converter can be realized by modulating the switching period. Normal PFM mode can be used in this condition. However, VS turn ON of switch cannot be guaranteed and the switching loss is unbearable. Thus, a PFM mode with fluctuation of switching period is used to realize VS turn ON of switch. The switching loss will be reduced greatly. To improve the efficiency further, an ON–OFF mode is applied to reduce the equivalent frequency, which automatically reduces the power losses.

V. EXPERIMENTAL RESULTS

A 1 MHz 12 V/3 A prototype with 80 V dc input voltage is established to verify the above analysis. The equivalent duty ratio D_{eq} is set as 0.5 at full load. The converter parameters are summarized in Table I. The test board is shown in Fig. 10. The length of the prototype is 93 mm, the width is 38 mm, and the height is 10 mm. Since the prototype is just established for experimental verification, the optimization of the converter volume is not considered at present. As the switching frequency is improved to 1 MHz, the volume of the proposed converter can be further reduced in the future.

A. Open-Loop Waveforms

The waveforms of open-loop test are verified in this part. Fig. 11 shows the waveforms of an open-loop test. i_p is the primary current. v_{ds} is the drain source voltage of the GaN switch, and v_{gs} is the driver signal of the switch. v_{Cr} is the voltage of the resonant capacitor. The switch is turned ON at

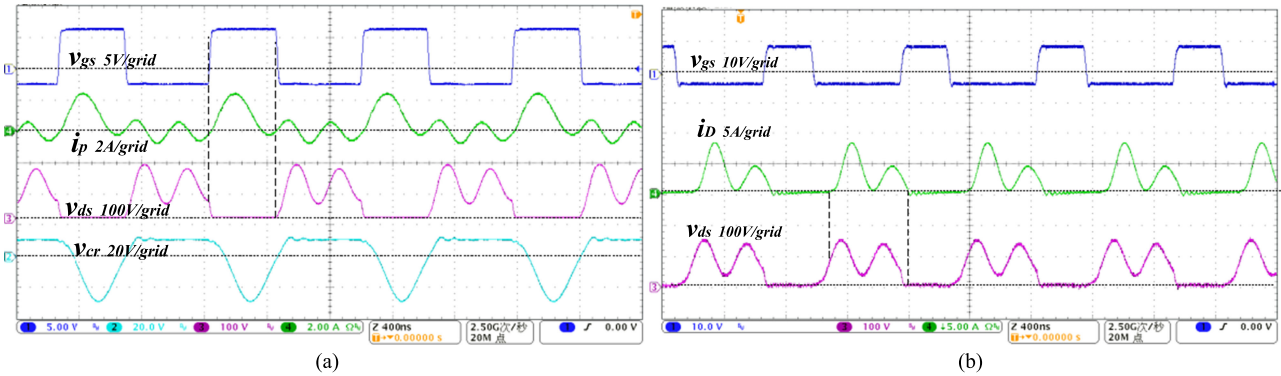

Fig. 11. Open-loop waveforms of the proposed topology. (a) ZCS turn OFF and VS turn ON of switch. (b) ZCS turn OFF of diode.

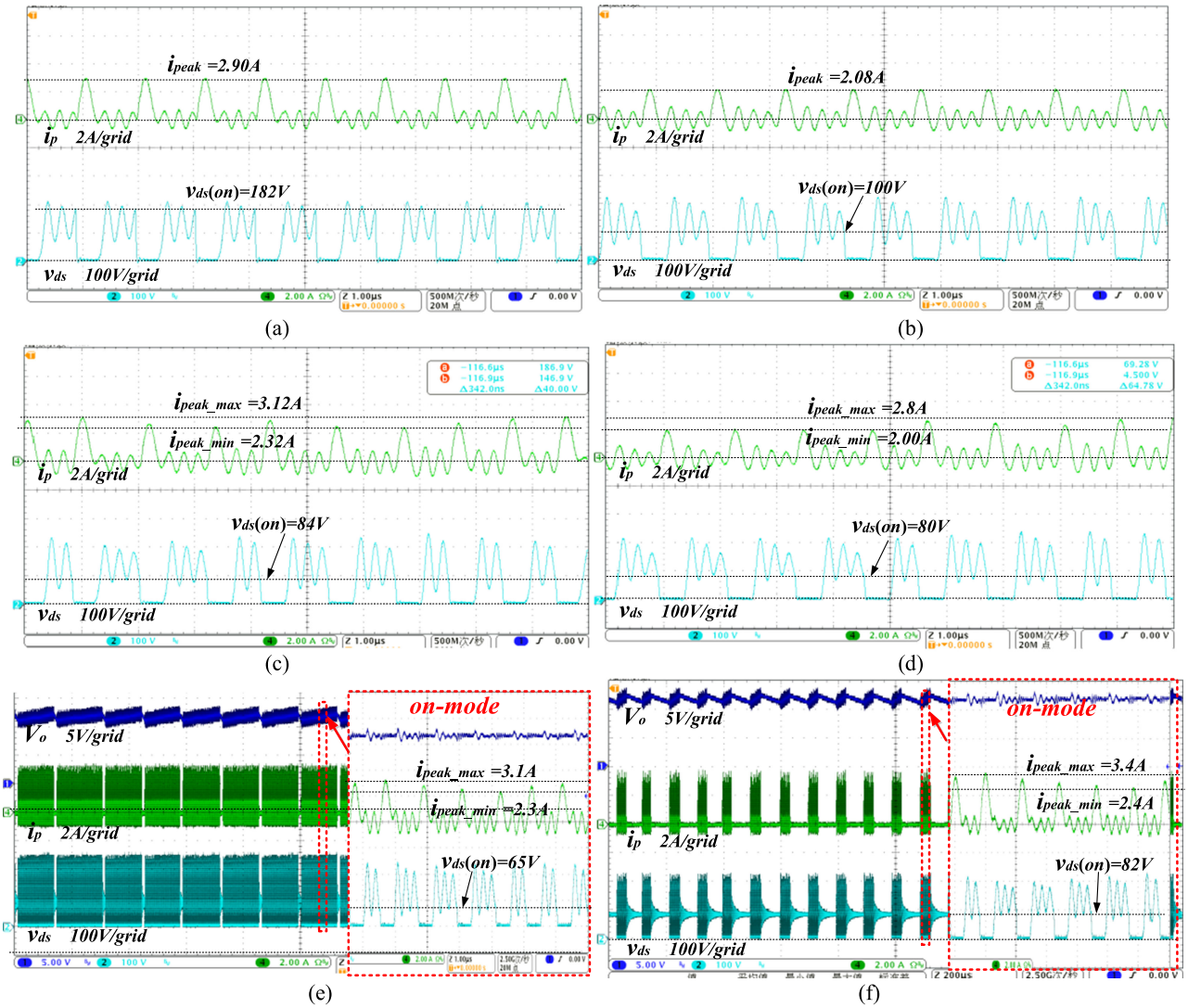

Fig. 12. Waveforms of different control modes. (a) Normal PFM mode when the load is 4 Ω. (b) Normal PFM mode when the load is 10 Ω. (c) PFM mode with fluctuation when the load is 4 Ω. (d) PFM mode with fluctuation when the load is 10 Ω. (e) ON–OFF mode using PFM mode with fluctuation when the load is 4 Ω. (f) ON–OFF mode using PFM mode with fluctuation when the load is 10 Ω.

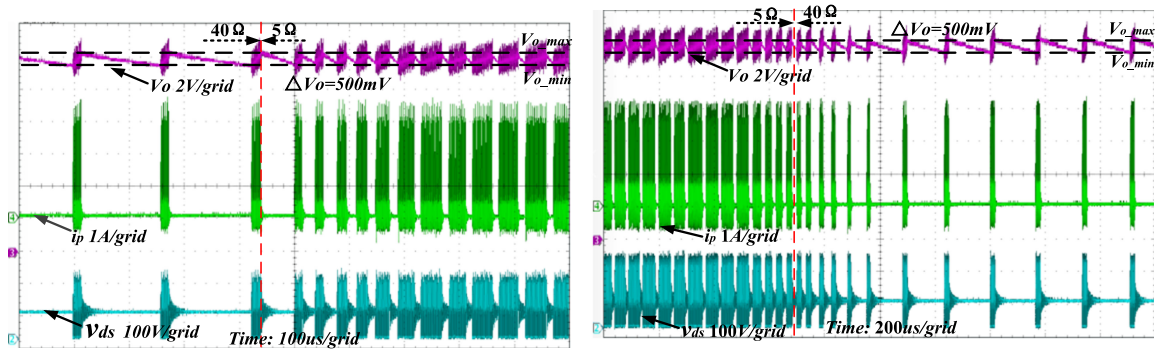

Fig. 13. Load transient response waveforms. (a) Load change from 40 to 5 Ω. (b) Load change from 5 to 40 Ω.

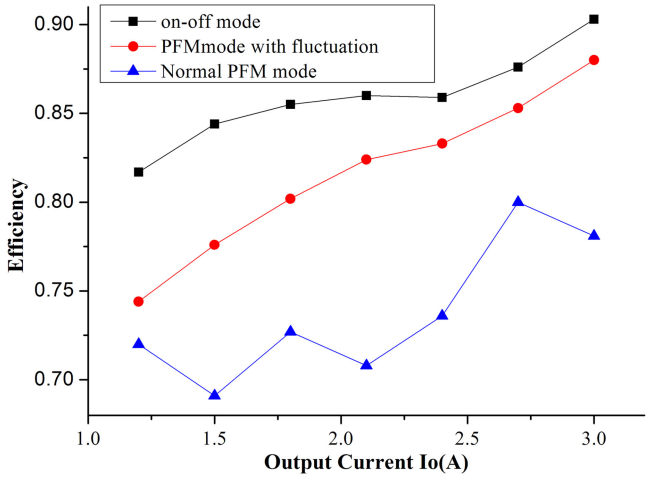

Fig. 14. Efficiency comparison between the three control methods.

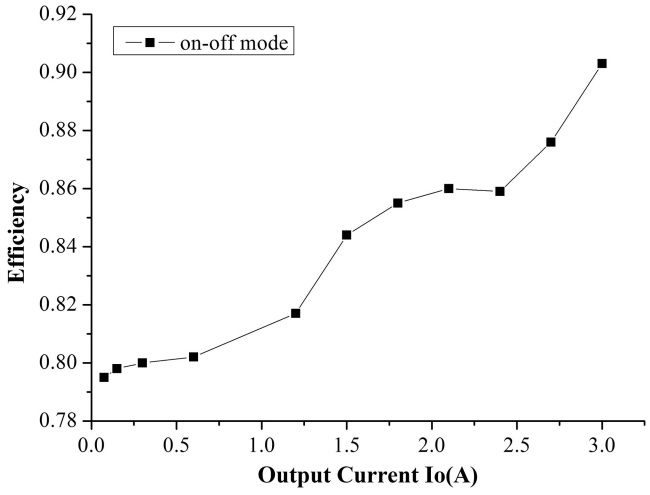

Fig.15. Total efficiency of ON–OFF mode.

the valley of $v_{\rm ds}$ and turned OFF at zero current. ZCS turn OFF and VS turn ON of switch and are realized. The switching loss is greatly reduced and *dv/dt* and *di/dt* values are both reduced. Additionally, the output diode is turned OFF at zero current; ZCS turn OFF of diode is achieved. Nearly fully soft switching is accomplished in the proposed converter.

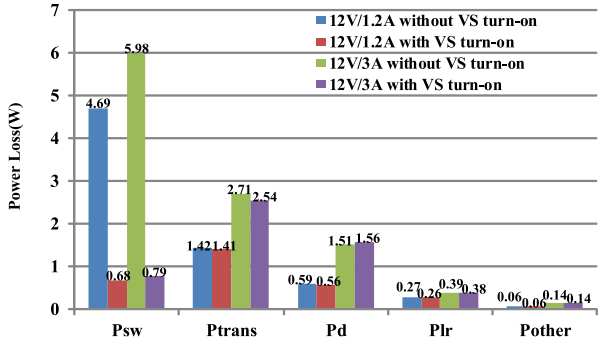

Fig. 16. Loss evaluation of normal PFM mode and PFM mode with fluctuation.

B. Closed-Loop Waveforms

The waveforms of closed-loop control methods including the two PFM mode and ON–OFF mode are compared in this part.

Fig. 12 shows the switch drain voltage $v_{\rm ds}$ and the primary winding current of two different loads when normal PFM mode is used to modulate the switching period. VS turn ON of switch cannot be guaranteed. When the load is 4 Ω, the primary peak current $i_{\rm peak}$ is 2.90 A and the switch is turned ON at the peak voltage of $v_{\rm ds}$. The average turn ON voltage of $v_{\rm ds}$ is 182 V. Thus, the switching loss is large in this condition. The efficiency is 74.1%. When the load becomes light, the magnetizing current decreases. As in Fig. 12(b), the primary peak current drops to 2.08 A and the turn ON voltage $v_{\rm ds}$(on) drops to 100 V when the load is 10 Ω.

When PFM mode with fluctuation of switching period is used, VS turn ON of switch can be guaranteed. Fig. 12(c) shows the switch drain voltage $v_{\rm ds}$ and the primary winding current i_p when the load is 4 Ω. The primary peak current $i_{\rm peak}$ varies from 2.32 to 3.12 A and the average turn ON voltage $v_{\rm ds}$(on) is 88 V. VS turn ON of switch is realized and the efficiency is 87.9%. When the load becomes light, the magnetizing current decreases. As in Fig. 12(d), when the load is 10 Ω, primary peak current $i_{\rm peak}$ varies from 2.32 to 3.12 A and the average turn ON voltage $v_{\rm ds}$(on) is 88 V. And the efficiency is dropped to 77.6%.

When ON–OFF mode using PFM mode with fluctuation is used, VS turn ON of switch is realized. The efficiency reaches 90.3% when the load is 4 Ω. As seen in Fig. 14(e), $i_{\rm peak}$ varies

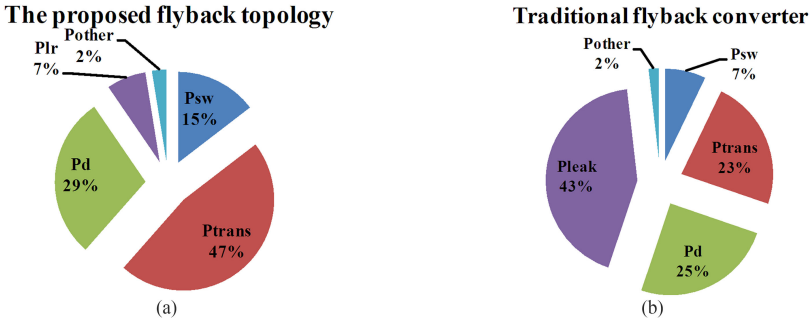

Fig. 17. Power loss comparison with traditional flyback converter. (a) Traditional flyback converter at 60 W. (b) Proposed converter at 36 W.

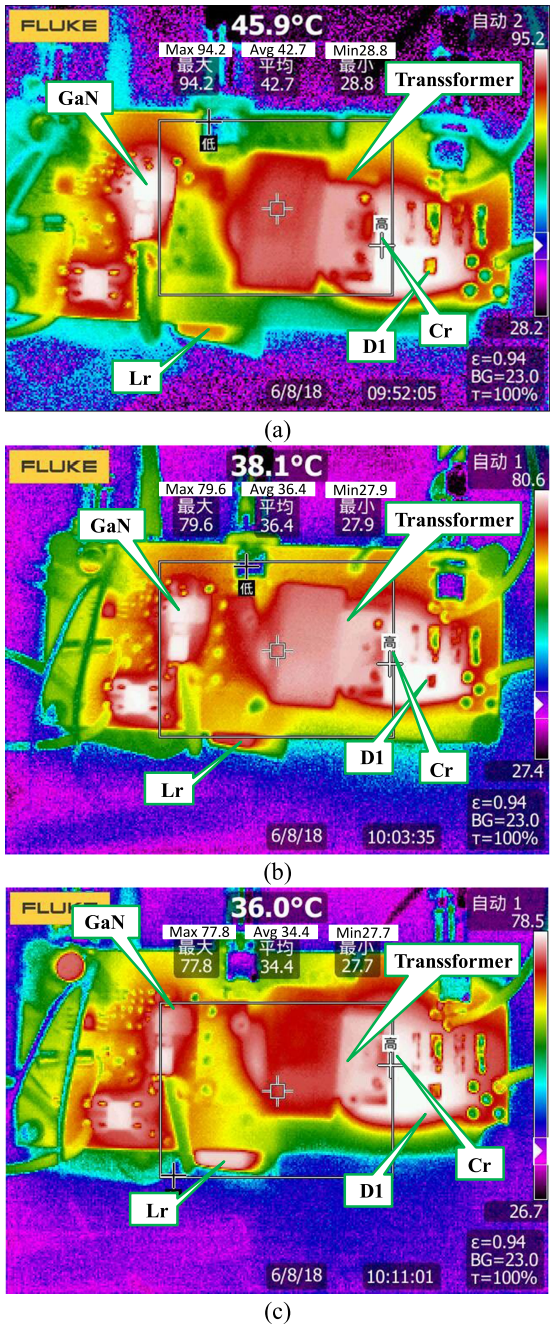

Fig. 18. Thermal images and associated prototypes at 36 W. (a) Normal PFM mode. (b) PFM mode with time fluctuation. (c) ON–OFF mode.

from 2.3 to 3.1 A when the load is 4 Ω. As seen in Fig. 14(f), $i_{\rm peak}$ varies from 2.4 to 3.4 A when the load is 10 Ω. During ON mode, as the magnetizing current varies around $I_{m\_\max}$, the primary peak current variation range is nearly the same.

The dynamic performance of ON–OFF mode can be shown in Fig. 13. As the output voltage is sampled by analog-to-digital converter (ADC) device. Almost no overshoot voltage or undershoot voltage is observed.

C. Efficiency Comparison

The efficiencies of the two PFM modes and the ON–OFF mode are shown in Fig. 13. They are compared in following part. The efficiency of PFM mode with fluctuation is larger than the efficiency of normal PFM mode as VS turn ON of switch is satisfied. In normal PFM mode, the switch is mostly turned ON when the drain voltage $v_{\rm ds}$ is at its high values. Thus, this switching loss is much higher than that of PFM mode with fluctuation.

In the two PFM modes, when the load becomes light, the conduction loss is reduced. The transformer core loss is nearly unchanged as variation of the magnetizing current in one switching cycle is almost unchanged. The diode conduction loss also keeps constant as the forward voltage is nearly constant. Thus, when load becomes light, the transformer core loss and the diode loss occupy the majority of total power loss and the efficiencies of the two PFM modes decrease. The efficiency fluctuation of normal PFM mode when load becomes light is mainly introduced by the fluctuation of the switch turn ON voltage [$v_{\rm ds}$(on)].

The efficiency of ON–OFF mode is larger than the efficiency of PFM mode with fluctuation, as the equivalent switching frequency is reduced. The peak efficiency is 90.3% in ON–OFF mode at full load. In ON mode period, the power efficiency in $t_{\rm rise}$ period is lower than the power efficiency in $t_{\rm stable}$ period. When the load becomes light, $t_{\rm rise}$ period of ON mode is constant and $t_{\rm stable}$ period of ON mode becomes short. Thus, the average power efficiency of ON mode will decrease when the load becomes light.

The total efficiency of ON–OFF mode from 0% to 100% load is shown in Fig. 15. The peak efficiency is 90.3% and the minimum efficiency is 79.2%.

The loss evaluations of normal PFM mode and PFM mode with fluctuation can be seen as in Fig. 16. Before VS turn ON of switch is realized in normal PFM mode, the switching loss $P_{\rm sw}$ occupies nearly half of the total loss. This is why the switching

TABLE II
COMPARISON WITH OTHER SINGLE SWITCH SOFT-SWITCHED CONVERTER

	[1]	[12]	[14]	[6]	This work
Topology type	Forward converter	Forward converter	Flyback converter	Flyback converter	Flyback converter
Circuit complexity	Complex	Simple	Simple	Complex	Simple
Soft-switching technique	ZCS turn-on, ZVS turn-off	ZCS turn-on, ZCS turn-off	ZCS turn-on, ZCS turn-off	VS turn-on, ZVS turn-off	VS turn-on, ZCS turn-off
Maximum switching frequency	100 kHz	300 kHz	500 kHz	340 kHz	1 MHz
Maximum output power	250 W	100 W	250 W	65 W	36 W
Maximum efficiency	97.0%	90.0%	92.5%	90.5%	90.3%

frequency is not improved to 1 MHz in traditional quasi-resonant flyback converter. The transformer loss $P_{\rm trans}$ are the main loss apart from the switching loss. The output diode loss P_d is also important, which is nearly proportional to the output current. The loss of the resonant inductor L_r is $P_{\rm lr}$ and the other loss is $P_{\rm other}$. $P_{\rm lr}$ and $P_{\rm other}$ are much smaller than other power losses. After VS turn ON of switch is realized in PFM mode with fluctuation, the switching loss is reduced greatly and the total loss is reduced a lot. Thus, the switching frequency can be improved. The transformer loss $P_{\rm trans}$ is the main part of the power losses. The switching loss $P_{\rm sw}$ and the output diode loss P_d are also important losses. The switching loss $P_{\rm sw}$ is nearly unchanged under different load. The output diode loss P_d is also important, which is nearly proportional to the output current. $P_{\rm lr}$ is much smaller than other power losses and the other loss $P_{\rm other}$ can be neglected.

As in Fig. 17, the power loss of the proposed converter is compared to that of traditional flyback converter. In traditional flyback converter [18], the power loss from the leakage inductance $P_{\rm leak}$ is the main part of the total loss, which is eliminated in the proposed converter. In the proposed flyback converter, the switching frequency increases, $P_{\rm trans}$ and $P_{\rm sw}$ increases, P_d is nearly constant. As the improvement of the switching loss $P_{\rm sw}$ is not large, the switching frequency can be improved up to 1 MHz. However, compared to traditional flyback converter, the proportions of $P_{\rm trans}$ and $P_{\rm sw}$ are increased at high switching frequency.

Thus, the peak efficiency of the proposed converter is lower than the peak efficiency of other low switching frequency converters. In the future, when synchronous rectification is used, P_d will be reduced a lot and the peak efficiency can be improved to nearly 93%.

Thermal images of the three closed-loop control methods are shown in Fig. 18. From the total temperature of the three conditions, the power loss of ON–OFF mode is the lowest and the power loss of normal PFM mode is the highest. The temperatures of the output diode D1, GaN MOSFET, and the transformer are high. From the temperature comparisons, the switching loss is reduced from normal PFM mode to PFM mode with time fluctuation as GaN device temperature is reduced from about 92° to 80°. Compared to PFM mode with time fluctuation, the transformer core loss and the switch loss of ON–OFF mode are reduced obviously. This verified the efficiency improvement of ON–OFF mode compared to that of PFM mode with time fluctuation.

D. Comparison With Other Works

This paper is compared with other single-switch soft-switched converters as in Table II. At turn ON of switch, ZCS turn ON can reduce the switching loss; but the power loss from the equivalent drain capacitor cannot be reduced. This drain capacitor loss will increase linearly with the switching frequency, and it will limit the increase of the switching frequency. Thus, VS turn ON or ZVS turn ON of switch is preferred as the drain capacitor loss will be reduced or removed and *dv/dt* value is attenuated; and the switching frequency can be improved further. At turn OFF of the switch, ZVS turn OFF can reduce the switching loss, but introduce large *di/dt* value. ZCS turn OFF can reduce the switching loss and reduce *di/dt* value. Thus, ZCS turn OFF of switch is preferred.

Compared to other works, the switching loss of the proposed work is smaller as VS turn ON of switch is realized; *dv/dt* and *di/dt* values of the proposed work are both small as VS turn ON and ZCS turn OFF of switch are accomplished. Besides, the circuit of the converter is very simple as it has very few components. While other similar works has more components and the cost is higher. The switching frequency is improved to 1 MHz and the peak efficiency is 90.3%. Compared to other single-switch soft-switched converters, high frequency, high efficiency, low switching noise, and low cost are all accomplished in the proposed topology.

The proposed single-switched high-switching-frequency quasi-resonant flyback converter is verified by a 1-MHz 12-V/3-A prototype with 80-V input. Soft switching including ZCS turn OFF and VS turn ON of switch and ZCS turn OFF of diode are achieved. Based on PFM mode with time fluctuation, VS can be realized. The switching loss is reduced and low *dv/dt* and *di/dt* values are obtained. The total efficiency is further optimized by ON–OFF mode compared to the two PFM modes.

VI. CONCLUSION

A single-switched quasi-resonant flyback converter with ZCS and VS of switch is proposed in this paper. A resonant

inductor of primary side and a resonant capacitor of secondary side are used to realize VS turn ON and ZCS turn OFF of switch and ZCS turn OFF of diode. Near fully soft switching is realized. Thus, very low cost and very high efficiency can be obtained. To realize closed-loop control and realize VS turn ON of switch, PFM mode with time fluctuation is applied for constant output voltage control. Based on PFM mode with fluctuation, an ON–OFF mode is used to improve the overall efficiency of the converter. The proposed concept has been validated on a 1-MHz 12-V/3-A prototype with 80-V dc input voltage using GaN MOSFET. VS turn ON and ZCS turn OFF of switch and ZCS turn OFF of diode are verified and the peak efficiency is 90.3% using ON–OFF mode. High frequency, high efficiency, low switching noise, and low cost are all accomplished in the proposed topology. The future work will focus on realization of synchronous rectification and improve the output power up to 100 W.

REFERENCES

[1] M. Kim and S. Choi, "A fully soft-switched single switch isolated DC-DC converter," *IEEE Trans. Power Electron.*, vol. 30, no. 9, pp. 4883–4890, Oct. 2014.

[2] M. Khalilian and E. Adib, "Soft-single-switch dual forward-flyback PWM DC-DC converter with non-dissipative LC circuit," in *Proc. Iranian Conf. Electron. Eng.*, 2015, pp. 1562–1567.

[3] E. Chung, K.-H. Lee, and Y. Han, "Single switch high frequency DC-DC converter using parasitic components," *IEEE Trans. Power Electron.*, vol. 32, no. 5, pp. 3651–3661, Jun. 2016.

[4] S.-H. Ryu, J.-H. Ahn, and B.-K. Lee, "Single-switch ZVZCS quasi-resonant CLL isolated DC-DC converter for 32" LCD TV," in *Proc. IEEE Energy Convers. Congr. Expo.*, 2013, pp. 4887–4893.

[5] Y. Kitano, H. Omori, and N. Kimura, "A new wireless EV charger using single switch ZVS resonant inverter with optimized power transfer and low-cost PFC," in *Proc. Int. Conf. Elect. Drives Power Electron.*, 2015, pp. 515–521.

[6] J. Li, F. B. M. van Horck, H. J. Bergveld, and B. Daniel, "A high-switching-frequency flyback converter in resonant mode," *IEEE Trans. Power Electron.*, vol. 32, no. 11, pp. 8582–8592, Nov. 2017.

[7] J.-M. Kwon, W.-Y. Choi, and B.-H. Kwon, "Single-stage quasi-resonant flyback converter for a cost-effective PDP sustain power module," *IEEE Trans. Ind. Electron.*, vol. 58, no. 6, pp. 2372–2377, Aug. 2010.

[8] K.-B. Park, C.-E. Kim, and G-W. Moon, "PWM resonant single-switch isolated converter," *IEEE Trans. Power Electron.*, vol. 24, no. 8, pp. 1876–1886, Aug. 2009.

[9] J. M. Kwon, W. Y. Choi, and B. H. Kwon, "Single-switch quasi-resonant converter," *IEEE Trans. Power Electron.*, vol. 56, no. 4, pp. 1158–1163, Oct. 2008.

[10] C. Y. Hsu and Y. L. Chang, "A single stage single switch valley switching flyback-forward converter with regenerative snubber and PFC for LED light source system," in *Proc. Int. Conf. Int. Green Building Smart Grid*, 2014, pp. 1–6.

[11] N. Quentin, R. Perrin, and C. Martin, "A single switch resonant and quasi-resonant converter suitable for low power applications," in *Proc. Annu. Conf. IEEE Ind. Electron. Soc.*, 2016, pp. 3196–3201.

[12] A. Emrani, E. Adib, and H. Farzanehfard, "Single-switch soft-switched isolated DC–DC converter," *IEEE Trans. Power Electron.*, vol. 27, no. 4, pp. 1952–1957, Apr. 2012.

[13] J.-Y. Lee, G.-W. Moon, and H.-J. Park, "Integrated ZCS quasi-resonant power factor correction converter based on flyback topology," *IEEE Trans. Power Electron.*, vol. 15, no. 4, pp. 634–643, Jul. 2000.

[14] F. Tian, F. Chen, and K. Rustom, "Pulse frequency modulation with soft-switching flyback signal-stage inverter," in *Proc. Intelec Conf.*, 2010, pp. 1–6.

[15] H. Sugimura, B. Saha, and H. Omori, "Single reverse blocking switch type pulse density modulation controlled ZVS inverter with boost transformer for dielectric barrier discharge lamp dimmer," in *Proc. Int. Power Electron. Motion Control Conf.*, pp. 1–5, 2006.

[16] A. Abasian, H. Farzaneh-Fard, and S. Madani, "Single stage soft switching ac-dc converter without any extra switch," *IET Power Electron.*, vol. 7, no. 3, pp. 745–752, Apr. 2014.

[17] B. Kang, K.-S. Low, and J. J. Soon, "Single-switch quasi-resonant DC–DC converter for a pulsed plasma thruster of satellites," *IEEE Trans. Power Electron.*, vol. 27, no. 6, pp. 4503–4513, Aug. 2017.

[18] C. Wang, S. Xu, and S. Lu, "A low-cost constant current control method for DCM and CCM in digitally controlled primary-side regulation flyback converter," *IEEE J. Emerg. Sel. Topics Power Electron.*, vol. 6, no. 3, pp. 1483–1494, Dec. 2017.

Authors' photographs and biographies not available at the time of publication.